

Relativistic hydrodynamics in close binary systems: Analysis of neutron-star collapse

G. J. Mathews and P. Marronetti

University of Notre Dame, Department of Physics, Notre Dame, Indiana 46556

J. R. Wilson

*University of California, Lawrence Livermore National Laboratory, Livermore, California 94550**and University of Notre Dame, Department of Physics, Notre Dame, Indiana 46556*

(Received 3 November 1997; revised manuscript received 16 March 1998; published 22 July 1998)

We discuss the underlying relativistic physics that causes neutron stars to compress and collapse in close binary systems as has been recently observed in numerical $(3+1)$ -dimensional general relativistic hydrodynamic simulations. We show that compression is driven by velocity-dependent relativistic hydrodynamic terms which increase the self-gravity of the stars. They also produce fluid motion with respect to the corotating frame of the binary. We present numerical and analytic results that confirm that such terms are insignificant for uniform translation or when the hydrodynamics are constrained to rigid corotation. However, when the hydrodynamics are unconstrained, the neutron star fluid relaxes to a compressed nonsynchronized state of almost no net intrinsic spin with respect to a distant observer. We also show that tidal decompression effects are much smaller than the velocity-dependent compression terms for stars with a realistic compaction ratio. We discuss why several recent attempts to analyze this effect with constrained hydrodynamics or an analysis of tidal forces do not observe compression. We argue that an independent test of this effect must include unconstrained relativistic hydrodynamics to a sufficiently high order so that all relevant velocity-dependent terms and their possible cancellations are included. [S0556-2821(98)05416-2]

PACS number(s): 95.30.Lz, 04.25.Dm, 47.75.+f, 97.60.Jd

I. INTRODUCTION

The physical processes occurring during the last orbits of a neutron-star binary are currently a subject of intense interest [1–14]. In part, this recent surge in interest stems from relativistic numerical hydrodynamic simulations in which it has been noted [1–3] that as the stars approach each other their interior density increases. Indeed, for an appropriate equation of state, our numerical simulations indicate that binary neutron stars collapse individually toward black holes many seconds prior to the merger. This compression effect would have a significant impact on the anticipated gravity-wave signal from merging neutron stars. It could also provide an energy source for cosmological gamma-ray bursts [3].

In view of the unexpected nature of this neutron star compression effect and its possible repercussions, as well as the extreme complexity of strong field general relativistic hydrodynamics, it is of course imperative that there be an independent confirmation of the existence of neutron star compression before one can be convinced of its operation in binary systems. In view of this it is of concern that the initial numerical results reported in [1–3] have been called into question. A number of recent papers [4–14] have not observed this effect in Newtonian tidal forces [4], first post-Newtonian (1PN) dynamics [5–9,14], tidal expansions [10–12], or in binaries in which rigid corotation has been imposed [13]. The purpose of this paper is to point out that none of these recent studies could or should have observed the compression effect which we observe in our calculations.

Moreover, this flurry of activity has caused some confusion as to the physics to which we attribute the effects observed in the numerical calculations. The present paper,

therefore, summarizes our derivation of the physics which drives the collapse. We illustrate how such terms have been absent in some Newtonian or post-Newtonian approximations to the dynamics of the binary system. We also present numerical results and analytic expressions which demonstrate how the compression forces result in an orbiting dynamical system from the presence of fluid motion with respect to the corotating frame. As such, they could not appear in an analysis of relativistic external tidal forces no matter how many orders are included in the tidal expansion parameter (e.g. [11,12]), unless self gravity from internal hydrodynamic motion is explicitly accounted for. The effect could not also arise in systems with uniform translation or rigid corotation.

The implication of the present study is that any attempt to confirm or deny the compression driving force requires an unconstrained, untruncated relativistic hydrodynamic treatment. At present, ours is still the only existing such calculation. Hence, despite claims to the contrary [4–14], the neutron star compression effect has not yet been independently tested.

Another confusing aspect surrounding the numerical results has been our choice of a conformally flat spatial three-metric for the solution of the field equations. Indeed, it has been speculated that this approximate gauge choice (in which the gravitational radiation is not explicitly manifested) may have somehow led to spurious results. A second purpose of this paper, therefore, is to emphasize that the compression driving terms are a completely general result from the relativistic hydrodynamic equations of motion. The advantages of the conformally flat condition are that the algebraic form of the compression driving terms is easier to identify and that the solutions to the field equations obtain a

simple form. It does not appear to be the case, however, that the imposition of a conformally flat metric drives the compression. It has been nicely demonstrated in the work of Baumgarte *et al.* [13] that conformal flatness does not necessarily lead to neutron-star compression.

II. THE SPATIALLY CONFORMALLY FLAT CONDITION

There has been some confusion in the literature as to the uncertainties introduced by imposing a conformally flat condition (henceforth abbreviated CFC) on the spatial three-metric. Therefore we summarize here some attempts which we and others have made to quantify the nature of this approximation.

The only existing strong field numerical relativistic hydrodynamics results in three unrestricted spatial dimensions to date have been derived in the context of the CFC as described in detail in [1–3].

We begin with the usual Arnowitt-Deser-Misner (ADM) (3+1) metric [16,17] in which there is a slicing of the spacetime into a one-parameter family of three-dimensional hypersurfaces separated by differential displacements in a timelike coordinate:

$$ds^2 = -(\alpha^2 - \beta_i \beta^i) dt^2 + 2\beta_i dx^i dt + \gamma_{ij} dx^i dx^j, \quad (1)$$

where we take Latin indices to run over spatial coordinates and Greek indices to run over four coordinates. We also utilize geometrized units ($G = c = 1$) unless otherwise noted. The scalar α is called the lapse function, β_i is the shift vector, and γ_{ij} is the spatial three metric.

In what follows, we make use of the general relation between the determinant of the four metric $g_{\alpha\beta}$ and the ADM metric coefficients

$$\det(g_{\alpha\beta}) = -\alpha^2 \det(\gamma_{ij}) \equiv \alpha^2 \gamma^2, \quad (2)$$

where $\gamma \equiv \sqrt{-\det(\gamma_{ij})}$.

The conformally flat metric condition simply expresses the three metric of Eq. (1) as a position dependent conformal factor ϕ^4 times a flat-space Kronecker delta

$$\gamma_{ij} = \phi^4 \delta_{ij}. \quad (3)$$

It is common practice (e.g. [18–20]) to impose this condition when solving the initial value problem in numerical relativity. It is the natural choice for our three-dimensional quasiequilibrium orbit calculations [2] which in essence seek to identify a sequence of initial data configurations for neutron-star binaries.

The reason conformal flatness is chosen most frequently for the initial value problem is that it simplifies the solution of the hydrodynamics and field equations. The six independent components of the three metric are reduced to a single position dependent conformal factor.

Since conformal flatness implies no transverse traceless part of γ_{ij} it can minimize the amount of initial gravitational radiation apparent in the initial configuration. However, in general the physical data still contain a small amount of pre-existing gravitational radiation. This has been clearly demonstrated in numerical calculations of axisymmetric black-

hole collisions [21]. In exact numerical simulations, the gravitational radiation appears as the time derivatives of the spatial three metric ($\dot{\gamma}_{ij}$) and its conjugate (the extrinsic curvature \dot{K}_{ij}) are evolved. The immediate evolution of the fields from conformally flat initial data is characterized by the development of a weak gravity wave exiting the system.

An estimate of the radiation content of initial data slices for axisymmetric black hole collisions has been made by Abrahams [22]. Even for high values of momentum, the initial slice radiation is always less than about 10% of the maximum possible radiation energy (as estimated from the area theorem).

Two questions then are relevant to our application of the CFC. One is the validity of this metric choice for the initial value problem, and the other is the effect on the system of the “hidden” gravitational radiation in the physical data.

Regarding the validity of the CFC one has a great deal of freedom in choosing coordinates and initial conditions as long as the initial space is Riemannian and the metric coefficients satisfy the constraint equations of general relativity [23]. Indeed, we have shown in [2] that exact solutions for the CFC metric coefficients can be obtained by imposing the ADM Hamiltonian and momentum constraint conditions. Nevertheless, in three dimensions a physical space is conformally flat if and only if the Cotton-York tensor vanishes [25,26]:

$$C^{ij} = 2\epsilon^{ikl} \left(R^j_k - \frac{1}{4} \delta^j_k R \right)_{;l}, \quad (4)$$

where R^j_k is the Ricci tensor and R is the Ricci scalar for the three space.

Equation (4) vanishes by fiat for the three-space metric we have chosen. However, conformally flat solutions for physical problems have only been proven [25,26] for spaces of special symmetry (e.g. constant curvature, spherical symmetry, time symmetry, Robertson-Walker, etc. [25]). Hence, the invocation of the CFC here and in other applications is an assumption. That is, it is a valid solution to the Einstein constraint equations, but does not necessarily describe a physical configuration to which two neutron stars will evolve. Nevertheless, this is a valid approximation as long as the nonconformal contributions from the $\dot{\gamma}_{ij}$ and \dot{K}_{ij} equations in the exact two-neutron star problem remain small. Indeed, numerical tests for an axisymmetric rotating neutron star [27] and a comparison of the CFC vs an exact metric expansion for an equal-mass binary [5] have indicated that conformal flatness is a good approximation when it can be tested.

As a related illustration, consider the Kerr solution for a rotating black hole. It is well known that the Kerr metric is not conformally flat. The close binaries we study have specific angular momentum only slightly greater than that of an extreme Kerr black hole. Also, they ultimately merge and collapse to a single Kerr black hole. Hence, an analysis of the Cotton-York tensor for a Kerr black hole is another indicator of the degree to which conformal flatness is a valid approximation for neutron-star binaries.

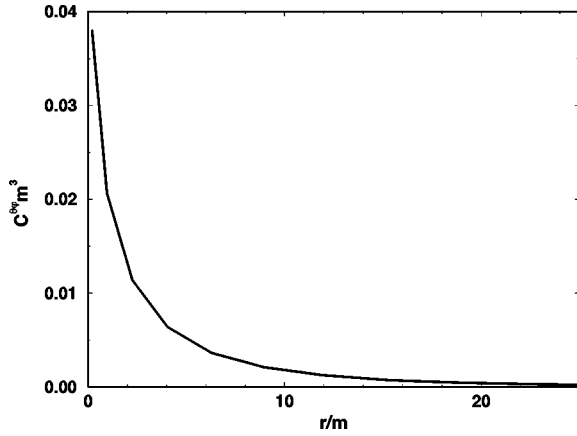


FIG. 1. The scaled Cotton-York tensor component $C^{\theta\phi}m^3$ as a function of the proper radius r/m for a maximally rotating $a=m$ Kerr black hole. This quantity is a measure of the deviation from conformal flatness.

Figure 1 gives the dimensionless scaled Cotton-York parameter $C^{\theta\phi}m^3$ for a maximally rotating Kerr black hole as a function of proper distance. For illustration, consider the decrease of this quantity as one moves away from the horizon at $m=r$ as a measure of the rate at which the metric becomes conformally flat. The maximally rotating ($a=m$) black hole of this example, however, is an extreme example of compactness and angular velocity relative to any of the neutron stars in our simulations.

It can be seen in Fig. 1 that, even for this extreme case, the dimensionless tensor coefficient $C^{\theta\phi}m^3$ diminishes rapidly away from the black hole. At the separation of interest for binary neutron stars approaching their final orbits ($r/m \sim 25$ where m is the total binary mass and r the separation between stars), this coefficient has already diminished to $\sim 10^{-3}$ of the value at the event horizon. Thus, the effect of either star on its companion is probably well approximated by conformal flatness. Regarding the interior of the neutron stars themselves, in our studies the stars are rotating so slowly (even when corotating) that the deviation from conformal flatness is probably negligible. Thus, it seems plausible that conformal flatness is a reasonable approximation for most physical aspects involving the spatial three-metric of binary neutron-star systems.

The next issue concerns the “hidden” radiation in the physical data. To address this we decompose the extrinsic curvature into longitudinal K_L^{ij} and transverse K_T^{ij} components as proposed by York [28]:

$$K^{ij} = K_L^{ij} + K_T^{ij}. \quad (5)$$

By definition the transverse part obeys

$$D_i K_T^{ij} = 0, \quad (6)$$

where D_i are covariant derivatives. The longitudinal part can be derived from a properly symmetrized vector potential. We find

$$D_i K_L^{ij} = 8\pi S^j, \quad (7)$$

where S^j are spatial components of the contravariant four-momentum density.

The product $K_T^{ij}K_{Tij}$ is a measure of the hidden radiation energy density. To then find K_T^{ij} from our numerical calculations, we first find K_{ij} by choosing maximal slicing [$Tr(K_{ij})=0$] and requiring that the trace free part of the $\dot{\gamma}_{ij}$ equation vanish. This gives [2]

$$2\alpha K_{ij} = (D_i \beta_j + D_j \beta_i - \frac{2}{3} \phi^{-4} \delta_{ij} D_k \beta^k). \quad (8)$$

We then determine K_L^{ij} from the equilibrium momentum density [Eq. (7)] and subtract K_L^{ij} from K^{ij} .

We find that this measure of the “hidden” gravitational radiation energy density is a small fraction of the total gravitational mass energy of the system:

$$\int K_T^{ij} K_{Tij} \frac{dV}{8\pi} \approx 2 \times 10^{-5} M_G. \quad (9)$$

Hence, we conclude that the CFC is probably a good approximation to the initial data.

This should be an excellent approximation for the determination of stellar structure and stability. However, an unknown uncertainty enters if one attempts to reconstruct the time evolution of the system (e.g. the gravitational waveform) from this sequence of quasistatic initial conditions. At present we make this connection approximately via a multipole expansion [24] for the gravitational radiation as described in [2].

A. An electromagnetic analogy

The meaning of imposing a conformally flat spatial metric can, perhaps, be qualitatively understood in an electromagnetic analogy. Both the ADM formulation of relativity and Maxwell’s equations can be written as two constraint equations plus two dynamical equations. In electromagnetism the constraint equations for electric and magnetic fields are embodied in the $\nabla \cdot E$ and $\nabla \cdot B$ equations, while the dynamical equations are contained in Ampere’s law and Faraday’s law. In relativity the analogous constraint equations are the ADM momentum and Hamiltonian constraints. The dynamical equations are the ADM \dot{K}_{ij} and $\dot{\gamma}_{ij}$ equations. In either electromagnetism or gravity, any field configuration which satisfies the constraint equations alone represents a valid initial value solution. However, one must analyze its physical meaning.

For example, consider two orbiting charges. One could construct an electric field that satisfies the constraint by simply summing over the electrostatic field from two point charges. Similarly, one can construct a static magnetic field from the charge current by imposing $\dot{E} = \dot{B} = 0$ in the dynamical equations. However, by forcing the dynamical equations to vanish, one has precluded the existence of electromagnetic radiation. In this field configuration, therefore one has unknowingly imposed ingoing radiation to cancel the outgoing electromagnetic waves.

Similarly, enforcing $\dot{K}_{ij} = \dot{\gamma}_{ij} = 0$ might in part be thought of as implying the existence of ingoing gravitational radiation.

tion to cancel the outgoing gravity waves. Nevertheless, in both cases, this remains a good approximation to the physical system (with no ingoing wave) as long as the energy density contained in the radiation is small compared to the energy in orbital motion.

Gravity waves enter in two ways: as estimated above there is an insignificant amount of “hidden” radiation induced by our choice of the CFC; there is also the emission of gravitational radiation by the orbiting binary system. The binary gravity-wave emission is estimated in our calculations by evaluating the multipole moments and using the appropriate formulas [2]. The fractional energy and angular momentum loss rate as determined by the multipole expansion method is quite small, e.g. $\dot{J}/\omega J \sim 10^{-4}$ in all of our calculations [2,3]. Hence, it can be concluded that the energy in gravitational radiation is indeed small compared to the energy in orbital motion.

The emission of gravity waves also induces a reaction force which we have incorporated into our hydrodynamic equations by the quadrupole formula. The radiation reaction force is so small, however, that it is difficult to discern it in the numerical results. In most of our calculations we simply neglect the back reaction terms and thereby obtain quasi-static orbit solutions.

B. Solutions to field equations

With a conformally flat metric, the constraint equations for the field variables ϕ , α , and β^i reduce to simple Poisson-like equations in flat space. The Hamiltonian constraint equation [17] for the conformal factor ϕ becomes [2,18]

$$\nabla^2 \phi = -2\pi\phi^5 \left[(1+U^2)\sigma - P + \frac{1}{16\pi} K_{ij} K^{ij} \right], \quad (10)$$

where σ is the inertial mass-energy density

$$\sigma \equiv \rho(1+\epsilon) + P, \quad (11)$$

and ρ is the local proper baryon density which is simply related to the baryon number density n , $\rho = \mu m_\mu n / N_A$, where μ is the mean molecular weight, m_μ the atomic mass unit, and N_A is Avogadro’s number. ϵ denotes the internal energy per unit mass of the fluid, and P is the pressure. In analogy with special relativity we have also introduced a Lorentz-like variable

$$[1+U^2]^{1/2} \equiv \alpha U^t = [1+U^j U_j]^{1/2} = [1+\gamma^{ij} U_i U_j]^{1/2}, \quad (12)$$

where U_i is the spatial part of the covariant four velocity. Here we explicitly write U^2 (in place of W^2-1 used in [1–3]) because it emphasizes the extra velocity dependence here and in the equations of motion.

In the Newtonian limit, the right-hand side of Eq. (10) is dominated [2] by the proper matter density ρ , but in relativistic neutron stars there are also contributions from the internal energy density ϵ , pressure P , and extrinsic curvature. This Poisson source is also enhanced by the generalized curved-space Lorentz factor $(1+U^2)$. This velocity factor

becomes important as the orbit decays deeper into the gravitational potential and the orbital kinetic energy of the binary increases.

It was pointed out in the Appendix of [3] that in analogy to the velocity-dependent enhancement of the source for Eq. (10), the Poisson source for the v^4 post-Newtonian correction to the effective potential also exhibits velocity-dependence. This appendix has been misinterpreted as a statement that we attribute the compression to a first post-Newtonian effect. We therefore wish to state clearly that the Appendix in that paper was merely an illustration of how the effective gravity begins to show velocity dependence even in a post-Newtonian expansion. The velocity dependence of the post-Newtonian source is not the main compression driving force. The compression derives mostly from the hydrodynamic terms described herein. It is not obvious, however, at what post-Newtonian order the compression effect should be counted, since different authors have treated these terms differently. We return to this point below.

In a similar manner [2], the Hamiltonian constraint, together with the maximal slicing condition, provides an equation for the lapse function:

$$\nabla^2(\alpha\phi) = 2\pi\alpha\phi^5 \times \left[3(U^2+1)\sigma - 2\rho(1+\epsilon) + 3P + \frac{7}{16\pi} K_{ij} K^{ij} \right]. \quad (13)$$

Here again, the source is strengthened when the fluid is in motion through the presence of a U^2+1 factor and the $K_{ij} K^{ij}$ term.

The momentum constraints [17] provide an elliptic equation [2] for the shift vector:

$$\nabla^2 \beta^i = \frac{\partial}{\partial x^i} \left(\frac{1}{3} \nabla \cdot \beta \right) + 4\pi \rho_3^i, \quad (14)$$

$$\rho_3^i = (4\alpha\phi^4 S_i - 4\beta^j(U^2+1)\sigma) \frac{1}{4\pi} \frac{\partial \ln(\alpha/\phi^6)}{\partial x^j} \times \left(\frac{\partial}{\partial x^j} \beta^i + \frac{\partial}{\partial x^i} \beta^j - \frac{2}{3} \delta_{ij} \frac{\partial}{\partial x^k} \beta^k \right), \quad (15)$$

where we have introduced [15] the Lorentz contracted coordinate covariant momentum density

$$S_i = \sigma W U_i. \quad (16)$$

As noted previously and in Ref. [2], we only solve Eq. (14) for the small residual frame drag after the dominant $\vec{\omega} \times \vec{r}$ contribution to $\vec{\beta}$ has been subtracted.

III. RELATIVISTIC HYDRODYNAMICS

The techniques of general relativistic hydrodynamics have been in place and well studied for over 25 years [15]. The basic physical processes which induce compression can be traced to completely general terms in the hydrodynamic equations of motion. To illustrate this we first summarize the

completely general derivation of the relativistic covariant momentum equation in Eulerian form and identify the terms that we believe to be the dominant contributors to the relativistic compression effect.

For hydrodynamic simulations it is convenient to explicitly consider two different spatial velocity fields. One is U_i , the spatial components of the covariant four velocity. The other is V^i , the contravariant matter three velocity, which is related to the four velocity

$$V^i = \frac{U^i}{U^t} = \frac{\gamma^{ij} U_j}{U^t} - \beta^i. \quad (17)$$

It is convenient to select the shift vector β^i such that the coordinate three velocity vanishes when averaged over the star, $\langle V^i \rangle = 0$. This minimizes the coordinate fluid motion with respect to the shifting ADM grid.

The perfect fluid energy-momentum tensor is

$$T_{\mu\sigma} = \sigma U_\mu U_\sigma + P g_{\mu\sigma}. \quad (18)$$

However, it is convenient to derive the hydrodynamic equations of motion using the mixed form

$$T_\mu{}^\nu = g^{\sigma\nu} T_{\mu\sigma} = \sigma U_\mu U^\nu + P \delta_\mu{}^\nu, \quad (19)$$

The vanishing of the spatial components of the divergence of the energy momentum tensor,

$$(T_i{}^\mu)_{;\mu} = 0, \quad (20)$$

leads to an evolution equation for the spatial components of the covariant four momentum:

$$\frac{1}{\alpha\gamma} \frac{\partial(S_i\gamma)}{\partial t} + \frac{1}{\alpha\gamma} \frac{\partial(S_i V^j \gamma)}{\partial x^j} + \frac{\partial P}{\partial x^i} + \frac{1}{2} \frac{\partial g^{\alpha\beta}}{\partial x^i} \frac{S_\alpha S_\beta}{S^t} = 0. \quad (21)$$

The covariant momentum equation is used because of its close similarity with Newtonian hydrodynamics. The first two terms are advection terms familiar from Newtonian fluid mechanics. The latter two terms are the pressure and gravitational forces, respectively.

Expanding the gravitational acceleration into individual terms we have

$$\begin{aligned} \dot{S}_i + S_i \frac{\dot{\gamma}}{\gamma} + \frac{1}{\gamma} \frac{\partial}{\partial x^j} (S_i V^j \gamma) + \frac{\alpha \partial P}{\partial x^i} - S_j \frac{\partial \beta^j}{\partial x^i} + \sigma \frac{\partial \alpha}{\partial x^i} \\ + \sigma \alpha \left(U^2 \frac{\partial \ln \alpha}{\partial x^i} + \frac{U_j U_k}{2} \frac{\partial \gamma^{jk}}{\partial x^i} \right) = 0. \end{aligned} \quad (22)$$

Similar forms can be derived for the condition of baryon conservation and the evolution of internal energy [2,15]. However, the above momentum equation is sufficient for the present discussion.

It is now worthwhile to consider the ‘‘gravitational’’ forces embedded in the expanded terms of Eq. (22). These result from the affine connection terms $\Gamma_{\mu\lambda}^\mu T^{\mu\lambda}$ in the covariant differentiation of $T^{\mu\nu}$.

The term containing $\partial\alpha/\partial x^i$ comes from the time-time component of the covariant derivative. It is of course the well-known analogue of the Newtonian gravitational force as can easily be seen in the Newtonian limit $\alpha \rightarrow 1 - Gm/r$.

The term $S_j(\partial\beta^j/\partial x^i)$ comes from the space-time covariant derivative. In an orbiting system it is convenient to allow β^j to follow the orbital motion of the stars. In our specific application [2] we let $\vec{\beta} = \vec{\omega} \times \vec{R} + \vec{\beta}_{resid}^{drag}$ where $\vec{\omega}$ is chosen to minimize matter motion on the grid. Hence, $\vec{\omega} \times \vec{R}$ includes the major part of rotation plus frame drag. The quantity $\vec{\beta}_{resid}^{drag}$ is the residual frame drag after subtraction of the rotation and is very small for the almost nonrotating stars that result from our calculations. With β^j dominated by $\vec{\omega} \times \vec{R}$, the term $S_j(\partial\beta^j/\partial x^i)$ is predominantly a centrifugal force.

The $U^2 \partial \ln \alpha / \partial x^i$ term arises from the time-time component of the affine connection piece of the covariant derivative. The $(U_j U_k / 2) \partial \gamma^{jk} / \partial x^i$ term similarly arises from the space-space components. They do not have a Newtonian analogue. As we shall see, these terms cancel when a frame can be chosen such that the whole fluid is at rest with respect to the observer (or in the flat space limit). However, for a star with fluid motion in curved space, they describe additional velocity-dependent forces.

We identify the nonvanishing combination of these U^2 -dependent force terms and the $S_j(\partial\beta^j/\partial x^i)$ term as the major contributors to the net compression driving force.

This suggests some useful test problems for our hydrodynamic simulations. For example, in simple uniform translation the effects of these terms must cancel to leave the stellar structure unchanged. Similarly, as discussed below, for any fluid motion, such that the four velocity can be taken as proportional to a corotating Killing vector, these force terms must cancel [13,25]. However, for more general states of motion, e.g. noncorotating stars, differential rotation, meridional circulation, turbulent flow, etc., these forces do not obviously cancel, but must be evaluated numerically.

Indeed, as discussed below, the sign of these terms is such that a lower energy configuration for the stars than that of rigid corotation can be obtained by allowing the fluid to respond to these forces. As we shall see, the numerical relaxation of binary stars from corotation (or any other initial spin configuration) produces a nonsynchronous (approximately irrotational) state of almost no intrinsic neutron-star spin in which the central density and gravitational binding energy increase.

A. Conformally flat relativistic hydrodynamics

The practical implementation of conformal flatness means that, given a distribution of mass and momentum, we first solve the constraint equations of general relativity at each time for a given distribution of mass-energy. We then evolve the hydrodynamic equations to the next time step. Thus, at each time slice we obtain a solution to the relativistic field equations and then can study the hydrodynamic response of the matter to these fields [2].

For the CFC metric, the relativistic momentum equation is derived by simply replacing $\gamma^{jk} \rightarrow \phi^{-4} \delta^{jk}$ in Eq. (22):

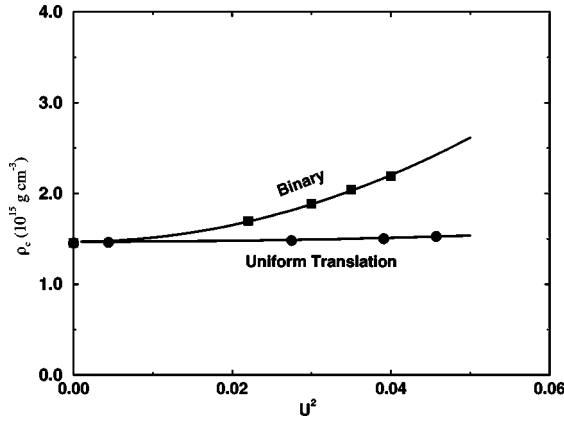


FIG. 2. Numerically evaluated central density for a uniformly translating star (lower curve) as a function of $U^2 \equiv U^i U_i$. This is compared with the central density for binary stars (upper curve) with the same average U^2 value. These calculations utilized the EOS of Ref. [2].

$$\begin{aligned} \frac{\partial S_i}{\partial t} + 6S_i \frac{\partial \ln \phi}{\partial t} + \frac{1}{\phi^6} \frac{\partial}{\partial x^j} (\phi^6 S_i V^j) + \alpha \frac{\partial P}{\partial x^i} - S_j \frac{\partial \beta^j}{\partial x^i} \\ + \sigma \frac{\partial \alpha}{\partial x^i} + \sigma \alpha U^2 \left(\frac{\partial \ln \alpha}{\partial x^i} - 2 \frac{\partial \ln \phi}{\partial x^i} \right) = 0. \end{aligned} \quad (23)$$

Here as in Eq. (22), the first term with $\partial \alpha / \partial x^i$ is the relativistic analogue of the Newtonian gravitational force.

In Eq. (23) there are two ways in which the effective gravitational force might increase for finite U^2 . One is that the matter contribution to the source densities for α or ϕ are increased by factors of $\sim 1 + U^2$ [cf. Eqs. (10) and (13)]. The more dominant effect, however, is from the combination of the $S_j \partial \beta^j / \partial x^i$ term and the $U^2 [\partial \ln \alpha / \partial x^i - 2 \partial \ln \phi / \partial x^i]$ terms in Eq. (23).

As noted previously, these compression driving terms result from the affine connection part $\Gamma_{\mu\lambda}^{\mu} T^{\mu\lambda}$ of the covariant differentiation of $T^{\mu\nu}$. These terms have no Newtonian analogue but describe a general relativistic increase in the gravitational force as U^2 increases. As noted in [2,3] (see also Fig. 2 below) for a binary, U^2 is approximately uniform over the stars, and the increase in central density due to these additional forces scales as $\approx U^4$. This scaling, however, is the net result from a nontrivial cancellation of terms and must be treated carefully. We shall return to this point below.

The proper way to determine the post-Newtonian order at which the compression driving terms enter would be to count the powers of c^2 that appear in the denominator of a term. For example, if we divide the last two terms in Eq. (23) by the gradient of the α term (the analogue of the Newtonian gravitational force) we would obtain a ratio of order U^2/c^2 which would be manifestly first post Newtonian. However, in the first post-Newtonian treatment of Wiseman [6], these velocity terms were explicitly disregarded. Thus, the effects of these terms could not have been present in that calculation. It is no surprise, therefore that no effect was observed in Ref. [6].

Also note that the $2 \partial \ln \phi / \partial x^i$ term in Eq. (23) enters with a sign such that the total U^2 -dependent contribution is fur-

ther increased by about twice that from the $\partial \ln \alpha / \partial x^i$ contribution alone. [The factor of 2 in front of the derivative comes from the requirement that $\phi^2 \sim (1/\alpha)$ in the Newtonian limit [2].]

A further increase of binding arises from the $K^{ij} K_{ij}$ terms in the field sources, but these terms are much smaller than the U^2 contributions for a binary system.

B. Comment on the relativistic Bernoulli equation

For comparison with other work in the literature it is instructive to discuss the derivation of the relativistic Bernoulli equation from Eq. (22). It has been pointed out (e.g. [13]) that the hydrodynamics reduce to a simple equation for a fluid in which the velocity field can be represented by a corotating Killing vector. In our notation this equation can be written

$$d \ln(U^t) = \frac{dP}{\sigma}. \quad (24)$$

The demonstration that the relativistic Bernoulli equation (24) is exactly reproduced from Eq. (22) when a corotating Killing vector can be imposed, was recently brought to our attention by Nakamura [29]. We summarize the derivation here in the conformally flat metric both for clarity and to show that conformal flatness does not violate this important constraint.

To begin with, note that in the ADM formalism, the existence of a Killing vector is equivalent to being able to choose the ADM shift vector such that $V^i = 0$ everywhere for the fluid. Next use Eq. (17) to solve for β^i and divide by σ . The resulting equation for stationary motion is

$$\frac{1}{\sigma} \frac{\partial P}{\partial x^i} = U^t U_j \frac{\partial}{\partial x^i} \left(\frac{U_j}{\phi^4 U^t} \right) - (\alpha U^t)^2 \frac{\partial \ln \alpha}{\partial x^i} + 2 U^2 \frac{\partial \ln \phi}{\partial x^i}. \quad (25)$$

The recovery of the relativistic Bernoulli equation requires that the right-hand side (RHS) $= \partial \ln U^t / \partial x^i$. With some straightforward algebraic manipulation it is possible to show that all of the terms on the RHS cancel except for one term from the β derivative, $-\phi^{-4} U^2 \partial \ln U^t / \partial x^i$. The completion of the proof is simply to note that this term is equal to $\partial \ln U^t / \partial x^i$ by Eq. (12). The result is Eq. (24).

It is instructive to consider the change in the relativistic Bernoulli equation when there is no Killing vector, i.e. $V^i \neq 0$. Along the same lines of the derivation of Eq. (25), it can be shown [29] that the momentum equation can be rewritten in our notation as

$$\begin{aligned} \frac{1}{\alpha \sigma} \left[\dot{S}_i + S_i \frac{\dot{\gamma}}{\gamma} + \frac{1}{\gamma} \frac{\partial}{\partial x^j} (S_i V^j \gamma) \right] + U^t U_j \frac{\partial V^j}{\partial x^i} \\ = - \frac{1}{\sigma} \frac{\partial P}{\partial x^i} + \frac{\partial \ln U^t}{\partial x^i}. \end{aligned} \quad (26)$$

The RHS is just the relativistic Bernoulli equation in the limit that the left-hand side (LHS) vanishes. In general fluid

flow, however, the LHS contains not only the advection terms (in brackets), but also an additional surviving part of the β^j derivative.

It can be seen from this that imposing a corotating Killing vector ($V^i=0$) means that only simple hydrostatic equilibrium is obtained for stationary systems. However, when non-trivial hydrodynamic motion is allowed, the extra forces embodied in the LHS of Eq. (26) are manifested. This leads to a deviation from the simple relativistic Bernoulli solution. Any attempt to model this deviation requires a careful treatment of the dynamical properties of the fluid described by the LHS of Eq. (26).

IV. CONSTRAINED HYDRODYNAMICS

Further insight into the complexity of the physics contained in the relativistic equations of motion can be gained by considering some simple examples of constrained hydrodynamics for which the answer is known. These pose useful tests of our numerical scheme. Since some have proposed that the effect we observe may be an artifact of numerical resolution or approximation, we present here a summary of various test problems designed to illustrate the stability of the numerics and also to compare with some of the calculations in the literature. These calculations also demonstrate that the compression effect vanishes in the limiting cases that have been studied by others. Hence, they could not have been observed. They highlight the fact that the effect we observe only appears in a strong field dynamic treatment which accounts for internal motion of stellar material in response to the binary and its effect on the star's self gravity. At present, ours may be the only existing result. This is consistent with the conclusion of [30] based upon test particle dynamics.

A. Bench mark calculations

To test for the presence of the compression driving forces we consider two bench-mark initial calculations. The bench mark of no compression is that of an isolated star. In our three dimensional hydrodynamic calculations, the single star structure is derived from Eq. (22) in the limit

$$S_i = U_i = V^i = \beta^i = 0. \quad (27)$$

The condition of hydrostatic equilibrium in isotropic coordinates is then trivially derived from Eq. (22):

$$\frac{\partial P}{\partial x^i} = -\sigma \frac{\partial \ln \tilde{\alpha}}{\partial x^i}, \quad (28)$$

where the tilde denotes that the metric coefficients are evaluated in the fluid rest frame. The Newtonian limit of the right hand side is recovered as $\tilde{\alpha} \rightarrow 1 - Gm/r$. Hence, we again identify the $\partial \ln \tilde{\alpha} / \partial x^i$ term with the relativistic analogue of the Newtonian gravitational force. Eq. (28) also trivially reduces to relativistic Bernoulli equation (24).

We have of course tested our three-dimensional calculations for single isolated stars. A single star remains stable on the grid indefinitely, except when the baryon mass exceeds

TABLE I. Central density for $m_B = 1.625M_\odot$ stars in various conditions using a $\Gamma = 2$ EOS.

Environment	Constraints	$\rho_c (10^{14} \text{ g cm}^{-3})$
Single star	Hydrostatic	5.84
Single star	Uniform translation	5.90
Binary	Tidal only	5.82
Binary	Rigid corotation	5.90
Binary	Rigid no spin	6.56
Binary	Full hydrodynamics	6.68

the maximum stable mass allowed by the Tolman-Oppenheimer-Volkov (TOV) equations. Above the maximum TOV mass the stars begin to collapse on a dynamical timescale as they should. We have also checked that the grid resolution used in our binary calculations is adequate to produce the correct central density, stellar radius, and gravitational mass of a single isolated star [3]. Hence, it seems unlikely that the inadequate grid resolution is the source of the compression effect as some have proposed.

In order to facilitate comparisons with the literature, and to avoid confusion over equation of state (EOS) issues, we have employed a simplistic $\Gamma = 2$ polytropic EOS, $P = K\rho^\Gamma$, where $K = 1.8 \times 10^5 \text{ erg cm}^3 \text{ g}^{-2}$. This gives a maximum neutron-star mass of $1.82M_\odot$. The gravitational mass of a single $m_B = 1.625M_\odot$ star in isolation is $1.51M_\odot$ and the central density is $\rho_c = 5.84 \times 10^{14} \text{ g cm}^{-3}$. The compaction ratio is $m/R = 0.15$, similar to one of the stars considered in [13]. Note that this EOS leads to stars with a lower compaction ratio than the stars we considered in [2,3] for which $m/R \approx 0.2$. Hence, the effects of tidal forces in the present calculations should be more evident.

The bench mark in which the compression is present is that of two equal mass stars in a binary computed with unconstrained hydrodynamics. The binary stars have the same baryon mass ($m_B = 1.625M_\odot$ each), the same EOS, and a fixed angular momentum $J = 2.5 \times 10^{11} \text{ cm}^2$ ($J/M_B^2 = 1.09$ where $M_B = 2m_B$). For these conditions the binary stars have $U^2 = 0.025$ and are at a coordinate separation of $\approx 100 \text{ km}$. The stars are stable but close to the collapse instability. Hence, they have experienced some compression that has increased their central density by 14% up to $\rho_c = 6.68 \times 10^{14} \text{ g cm}^{-3}$.

The central densities of these two bench marks are summarized in the first and last entries of Table I. To compare with these bench-mark calculations we have computed equilibrium configurations for stars under the various conditions outlined below. The test for the presence or absence of compression inducing forces will be the comparison of the numerically computed central density with that of a single isolated star or stars in a binary.

B. Stars in uniform translation

As a first nontrivial test, now consider a star as seen from an observer in an inertial frame which is in uniform transla-

tion with respect to the fluid. Choosing the motion to be along the x coordinate, the fluid three velocity is

$$\frac{U^x}{U^t} = V^x = \text{const.} \quad (29)$$

However, the observer is still free to choose the ADM shift vector such that the computational grid remains centered on the star. That is, although $S_i, U_i \neq 0$, we can still choose $V^i = 0$. This gives a restriction on β^i from Eq. (17):

$$\beta^x = \frac{\gamma^{xx} \alpha U_x}{W}. \quad (30)$$

Note, that this is an ADM coordinate freedom. It is not equivalent to a coordinate boost. It is in fact a Killing vector which is convenient for numerical hydrodynamics. It allows the matter to remain centered on the grid even though the equations of motion are being solved for fluid which is not at rest with respect to the observer.

With $V^i = 0$, the x component of the momentum equation (in equilibrium) becomes

$$\frac{\partial P}{\partial x} = \frac{S_x}{\alpha} \frac{\partial \beta^x}{\partial x} - \sigma \left[(U^2 + 1) \frac{\partial \ln \alpha}{\partial x} + \frac{U_j U_k}{2} \frac{\partial \gamma^{jk}}{\partial x} \right]. \quad (31)$$

With a CFC metric this becomes

$$\frac{\partial P}{\partial x} = \frac{S_x}{\alpha} \frac{\partial \beta^x}{\partial x} - \sigma \left[(U^2 + 1) \frac{\partial \ln \alpha}{\partial x} - 2U^2 \frac{\partial \ln \phi}{\partial x} \right]. \quad (32)$$

There are now several differences between this expression and that for an observer in the fluid rest frame. For one, there is the shift vector derivative $\partial \beta^x / \partial x$. Even in uniform translation this derivative is nonzero due to the variations of the metric coefficients over the star [cf. Eq. (30)]. Also, the effective gravity is enhanced by the $(U^2 + 1)$ velocity factor. The $U_j U_k / 2 \partial \gamma^{jk} / \partial x^i$ term also appears. In addition, the effective source terms (10) and (13) for the CFC metric coefficients are enhanced both by $(U^2 + 1)$ factors and the $K_{ij} K^{ij}$ term.

In spite of these differences, we nevertheless know that the locally determined pressure and inertial density must be the same as those determined for a star at rest. Indeed, since we can choose a Killing vector ($V^i = 0$) these equations must reduce to the relativistic Bernoulli equation (24).

Thus, this is an important numerical test problem. We solve the full hydrodynamic equations explicitly, e.g. Eq. (23), under the initial condition of nonzero U_x for a single star. The cancellations embedded in the hydrodynamics are not obvious. Nevertheless, in the end, all of these effects must cancel to leave the stellar central density unchanged (except for a Lorentz contraction factor).

To solve the uniform translation problem numerically we have applied the Hamiltonian and momentum constraints to determine the metric coefficients. We then evolved the full hydrodynamic equations to equilibrium. Figure 2 shows the numerically evaluated central density for such translating stars as a function of U^2 . These stars were calculated with the EOS of [2]. This is compared with the central density for

binary stars evolved at the same U^2 value using the same EOS. One can see that the translating stars maintain a constant central density (within numerical error) as they should. In contrast, the central density of binary stars grows as $\approx U^4$. This growth is the nontrivial net result from the velocity dependent terms in Eq. (23). It is not obvious, however, to what post-Newtonian order this dependence corresponds.

As summarized in Table I, the central density for a uniformly translating $\Gamma = 2$ star with $U^2 = 0.025$ (for comparison with the binary bench-mark calculation) is $5.90 \times 10^{14} \text{ g cm}^{-3}$. Within numerical accuracy, this central density is identical with that of an isolated star at rest.

This is at least indicative that our observed growth in central density may not be a numerical error as some have suggested (e.g. [10,12,30]). Such an error would likely be apparent in this test case. We argue that the difference between simple translation and binary orbits relates to the physics of the binary system itself, in particular physics which is not apparent in uniform translation, an analysis of tidal forces, or a truncated expansion that does not contain sufficient terms to adequately describe the dynamical response of the fluid.

C. Tidal forces

It has been pointed out [4,11,12] that tidal forces are in the opposite sense to the compression driving forces discussed here. That is, tidal forces distort the stars and decrease the central density and therefore render the stars less susceptible to collapse. We have argued [3] that although such stabilizing forces are present in our calculations they are much smaller in magnitude than the velocity-dependent compression driving terms. Nevertheless, the evolution of the matter fields in a calculation in which only tidal forces are present still represents a useful test of our numerical results. Stars in which only tidal forces act, should be stable and the central density should decrease rather than increase as the stars approach.

To test the effects of tidal forces alone we have constructed an artificial test calculation in which we place stars on the grid in a binary, but with no initial angular or linear momentum, i.e. $J = 0$ and $U^2 = 0$. This initial condition would normally evolve to an axisymmetric collision between the stars. However, after updating the matter fields, we artificially return the center of mass of the stars to the same fixed separation after each time step. We also reset to zero the mean velocity component directed along the line between centers. This sequence is repeated until the matter fields come to equilibrium. Since the velocity dependent forces eventually vanish, the only remaining forces are the pressure and static gravitational (including tidal) forces.

Results as a function of separation distance are shown in Table II for the $\Gamma = 2$ EOS and Table III for the realistic EOS used in [2]. For the realistic EOS the central density indeed decreases as the stars approach, consistent with the expectations from Newtonian and relativistic tidal analyses [4,12]. For the $\Gamma = 2$ polytropic EOS, the central density also decreases as the stars approach and remain below the central density of an isolated star. The fact that this table is not

TABLE II. Central density vs coordinate separation between centers for $m_B = 1.625 M_\odot$ ($\Gamma = 2$) stars in which only tidal forces are included. The neutron star radius (in isotropic coordinates) is 12 km.

Separation (km)	$\rho_c (10^{14} \text{ g cm}^{-3})$
41.8	5.821
50.6	5.816
81.8	5.821
∞	5.837

monotonic at the innermost point, however, may be due to a limitation of this numerical approximation for tidal forces as the ratio of separation to neutron-star radius diminishes.

Although the tidal forces do indeed stabilize the stars, their effect on the central density is quite small ($\sim 0.2\%$ decrease) compared to the net increase in density caused by the compression forces present for the binary. This is consistent with the relative order-of-magnitude estimates for these effects described in [3].

D. Stars in rigid corotation

As a next nontrivial example, consider stars in a binary system that are restricted to rigid corotation. In a recent series of papers, Baumgarte *et al.* [13] have studied neutron-star binaries using the same conformally flat metric. Their work differs from ours in that rather than solving the hydrodynamic equations, they describe the four velocity field by a Killing vector whereby the stars are forced to corotate rigidly. They also impose spatial symmetry in the three Cartesian coordinate planes so that they can solve the problem in only one octant. One should keep in mind, however, that rigid corotation is not necessarily the lowest energy configuration or the most natural [32] final state for two neutron stars near their final orbits. This assumption, though artificial, is nevertheless a means to constrain and simplify the fluid motion degrees of freedom. It is much easier to implement and therefore becomes an interesting test problem for codes seeking to explore the true hydrodynamic evolution of close binaries.

Indeed, it is possible to show [25] that in this limit, the neutron star hydrostatic equilibrium can be described by a simple Bernoulli equation in which the compression driving force terms are absent except for a weak velocity dependence. Analytically, the reason for this is trivially obvious from Eq. (26). The existence of a corotating Killing vector is

TABLE III. Same as Table II but for the EOS of Ref. [2]. The neutron star radius (in isotropic coordinates) is 6 km.

Separation (km)	$\rho_c (10^{14} \text{ g cm}^{-3})$
31.2	14.15
37.4	14.16
64.8	14.20
103.8	14.25
∞	14.30

equivalent to setting $V^i = 0$ globally. Choosing the ADM coordinates to remain centered on the stars, in steady state the time derivatives vanish along with the rest of the LHS of Eq. (26). Only the relativistic Bernoulli equation (24) survives.

It is not surprising, therefore that in [13] it has been demonstrated that in this special symmetry, the central density of the stars does not increase (within numerical error) as the stars approach the inner most stable circular orbit. In very close orbits the density actually decreases relative to the central density of stars at large separation. They also find that the orbit frequency remains close to the Newtonian frequency. Both of these results are interesting in that they confirm that the compression effect does not occur (as it should not) in this special symmetry. They also demonstrate that conformal flatness is not the source of the compression.

Accepting the results of [13] as correct, this then becomes another important test of our calculations. That is, if we artificially impose rigid corotation, then the central density should remain nearly constant until the stars are close enough that tidal effects cause the central density to decrease rather than increase.

Imposing rigid corotation, however, is not a trivial test problem to implement without completely replacing the hydrodynamic equations with the corresponding Bernoulli solution of [13,25]. (Indeed, we have done this [31] and reproduce the results of [13] quite well.) Moreover, we have found that directly modifying the hydrodynamic equations in an attempt to mimic a dynamically unstable configuration is difficult. One might think that the simplest way to implement corotation would be to impose a high fluid viscosity. Indeed high viscosity would resist the hydrodynamic forces described herein. However, a high fluid viscosity also resists the much weaker tidal forces and prevents the numerical relaxation to quasistatic equilibrium. It is thus difficult to achieve tidal locking by simply increasing the viscosity.

Instead, we introduce artificial forces on the fluid which continually drive the system toward a state of rigid corotation while allowing the system to at least somewhat respond hydrodynamically. To do this we define accelerations $(\dot{U}_i)_{\text{Rigid}}$ necessary to achieve rigid rotation by

$$(\dot{U}_i)_{\text{Rigid}} = \frac{(\tilde{U}_i - U_i)}{\Delta t} \quad (33)$$

where \tilde{U}_i are components of the rigidly corotating covariant four velocity in the $x-y$ orbit plane. These are determined by requiring that $\beta^i = (\omega \times r)^i$ and setting $V^i = 0$ in Eq. (17):

$$\tilde{U}_y = \frac{\omega x \phi^4}{\alpha \sqrt{1 - \omega^2 R^2 \phi^4 / \alpha^2}}, \quad (34)$$

$$\tilde{U}_x = \frac{-\omega y \phi^4}{\alpha \sqrt{1 - \omega^2 R^2 \phi^4 / \alpha^2}}, \quad (35)$$

where R is the coordinate distance from the center of mass of the binary.

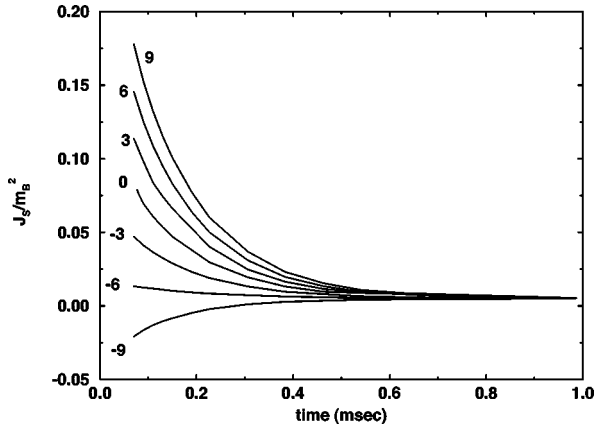


FIG. 3. Intrinsic neutron star spin J_S/m_B^2 as a function of coordinate time. The curves are labeled by the initial angular velocity ω_S (in units of 100 rad sec^{-1}) relative to the corotating frame.

At each time step we then update the momentum density using a combination of the hydrodynamic and corotating acceleration terms,

$$\dot{U}_i = f(\dot{U}_i)_{\text{Rigid}} + (1-f)(\dot{U}_i)_{\text{Hydro}}, \quad (36)$$

where $(\dot{U}_i)_{\text{Hydro}}$ is the acceleration from the full hydrodynamic equation of motion [Eq. (23)].

Numerically, we find that if f is small (<0.2) the hydrodynamic forces dominate and corotation is not obtained. On the other hand, for $f > 0.2$ the system is not stable, i.e. the stars deform and the velocities become erratic. We have therefore run with $f=0.2$ that temporarily produces a velocity field which is close to rigid corotation. That is, the residual three velocities are damped to a fraction of the orbit speed. This is, perhaps, good enough to make qualitative comparisons with the expectations from a truly corotating system.

Starting from the unconstrained initial configuration, we find that when the stars have achieved approximate corotation, the central density has decreased from $6.68 \times 10^{14} \text{ g cm}^{-3}$ to $5.90 \times 10^{14} \text{ g cm}^{-3}$ which is close to the value for stars in isolation ($5.84 \times 10^{14} \text{ g cm}^{-3}$). The calculated gravitational mass is slightly greater than that of the unconstrained binary. However, with the large artificial force terms needed to approximate corotation, gravitational mass is not a well defined quantity in this simulation. Also, the orbit frequency was not sufficiently converged for a meaningful comparison.

E. The spin of binary stars

As noted above our simulations indicate that neutron stars relax to a state of almost no intrinsic spin. In a separate paper [33] we analyze the nature and formation of this state in more detail. For the present discussion, however, we summarize in Fig. 3 a study of the relaxation to this state from states of arbitrary initial rigid rotation (including corotation).

As a means to distinguish the intrinsic spin motion of the fluid with respect to a non-orbiting distant observer, we define a quantity which is analogous to volume averaged intrinsic

stellar spin in the orbit plane,

$$J_S = \sum_{i=1,2} \int [(x-\tilde{x}_i)S_y - (y-\tilde{y}_i)S_x] \frac{\phi^2}{\alpha} dV_i, \quad (37)$$

where $(\tilde{x}_i, \tilde{y}_i, \tilde{z}_i=0)$ is the coordinate center of mass of each star.

In this study we have imposed an initial angular velocity ω_S in the corotating frame to obtain various initial rigidly rotating spin angular momenta (including corotation, $\omega_S=0$), but for fixed total $J/M_B^2=1.4$. We have considered spin angular frequencies in the range $-900 < \omega_S < 900 \text{ rad sec}^{-1}$, corresponding to $-0.03 < J_S/m_B^2 < 0.17$. We then let the system evolve hydrodynamically with the stars maintained at zero temperature.

In Ref. [3] we showed that the neutrino emission is sufficient to radiate away the released gravitational energy and keep the stars at near zero temperature until just before the collapse. This is the reason that we have treated this as a relaxation problem. That is, unlike a true hydrodynamic calculation, the relaxation calculation presented here, assumes that the stars radiate efficiently and stay at zero temperature. Therefore, this evolution does not need to conserve energy or circulation. This relaxation assumption is the reason the stars can evolve to a different spin (lower energy) state without violating the circulation theorem.

Figure 3 shows the spin J_S/m_B^2 as a function of time for each initial condition. In each case, the system relaxed to a state of almost no net spin within about three sound crossing times ($t \sim 0.6 \text{ msec}$). These calculations suggest that rapidly spinning neutron stars in close orbits are unstable. The true evolution time, however, would be much longer.

We also note that the quantity $\int \sigma[\sqrt{1+U^2}-1]dV$ decreased as the system evolved from rigid rotation to hydrodynamic equilibrium. Since this quantity is related to the kinetic energy of the binary, this indicates that the hydrodynamic lowest energy state is one of lower kinetic energy (for fixed total angular momentum) than that of rigid rotation.

As far as the compression effect is concerned, one wishes to know whether the response of the stars is simply due to that fact that they have no spin (and therefore no internal centrifugal force to support them against the compression forces), or whether more complex fluid motion within the star itself affects the stability. To test this, we have constructed stars of no spin ($J_S=0$) by simply damping the residual motion to that of $J_S=0$ after each update of the velocity fields.

Since this no-spin state is so close to the true hydrodynamic equilibrium, this produced stable $J_S=0$ equilibrium stars for the binary. For this case, the central density converges to $\rho_c = 6.56 \times 10^{14} \text{ g cm}^{-3}$ which is very close to the high value for the unconstrained hydrodynamics. This result would seem to indicate that most of the increase in density can be attributed to the velocity with respect to the corotating frame generated by the fact that the stars have almost no spin.

V. DISCUSSION

For clarity, we summarize in this section our conclusions regarding why the neutron-star compression effect was not observed in some other recent works.

First consider post-Newtonian expansions. In the work of Wiseman [6] the force terms containing U^2 were explicitly deleted from the computation of the stellar structure [cf. Eq. (8) in that paper]. Only the $d\ln\alpha/dx$ term was included. The recovery of simple hydrostatic equilibrium was thus unavoidable.

The PN orbiting ellipsoids of Shibata *et al.* [7] included more terms. Indeed, it was noted that there are two effects at 1PN order. One is the self gravity of each star of the binary and the other is the gravity acting between the stars. In their calculations the self gravity dominates causing the stars to become more compact. This is consistent with the compression effect described here in the sense that relativistic corrections can dominate over Newtonian tidal forces. However, the self gravity terms in [7] appear to only include the usual 1PN terms which would equally apply to stars in isolation. Hence, the velocity-dependent compression driving terms are probably not present.

Their results for stars in corotation are consistent with ours under the same constraint. They also note that approaches in which PN corrections to the gravity between the stars are included without also including the corrections to the self gravity (as in [9]) can be misleading.

In the work of Lombardi *et al.* [8] both corotating and irrotational equilibria were computed. However, in their calculations it appears that the stars become less compact as they approach contrary to our results and the results of [7]. It may be that the reason for this is that in Lombardi *et al.* the post-Newtonian corrections to self gravity were only computed for stars “instantaneously at rest.” The authors chose to “exclude the spin kinetic energy contribution to the self energy.” It is such terms, however, that we identify with the compression effect.

The conformally flat corotating equilibria computed by Baumgarte *et al.* [13] are consistent with our results. Since their stars were restricted to rigid corotation, only the hydrostatic Bernoulli solution would result. They could not have observed the compression forces which result from fluid motion with respect to the corotating frame.

We have argued in this paper that if one wishes to explore this effect, it would be best to apply a complete unconstrained strong-field relativistic hydrodynamic treatment for stars which are not in corotation. In this regard, a recent paper [14] has come to our attention in which hydrodynamic simulations of both corotating and irrotational binaries have been studied in a first post-Newtonian approximation to conformally-flat gravity but using the full relativistic hydrodynamics equation (22). For both corotational and irrotational stars the central density is observed to oscillate about a value which is less than that of isolated stars. Hence, the authors conclude that no compression effect is present.

Since this calculation contains many of the higher order terms to which we attribute the compression effect, it is not immediately obvious why the compression effect was not

observed. This may indeed be a real contradiction. We suggest, however, that this simulation did not observe the effect because of their use of an unrealistically soft $\Gamma = 1.4$ EOS. The authors chose this EOS because the stars become so extended that one can compute arbitrarily close binaries without encountering the relativistic inner orbit instability. For the irrotational stars (model *Bc* in [14]), which is the only simulation that might have observed the compression effect, the compaction ratio is only $M/R = 0.023$. Hence, a $1.45 M_\odot$ neutron star would have an unrealistic radius of 93 km.

However, since they have simulated very extended stars at very close separation, the tidal forces are much stronger relative to the relativistic compression driving terms than in any of the simulations which we have done.

The ratio of the stabilizing tidal correction ΔE_{tidal} to the destabilizing energy from compression ΔE_{comp} should scale [3,4] as

$$\frac{\Delta E_{tidal}}{\Delta E_{comp}} \propto \left(\frac{R}{r}\right)^6, \quad (38)$$

where R is the neutron star radius and r is the orbital separation. For model *Bc* in [14] we estimate that this ratio is ≥ 200 times greater than any of the binary stars we have considered. Hence, it is quite likely that the authors have simply chosen an unrealistically soft equation of state for which the tidal forces dominate over compression. It might be very interesting to see the results from a similar study for stars with a realistic compaction ratio and several radii apart.

Concerning tidal expansions, in Brady and Hughes [10] an attempt was made to analyze the stability of a central star perturbed by an orbiting point particle. The metric and stress-energy were perturbed in terms of order $\epsilon = \mu/R$ where μ is the point particle mass and R its coordinate distance from the central star. The Einstein equation was then linearized to terms of order ϵ . The result of this linearization was that the only possible correction to the central density was a single monopole term of order $\mu/R \sim v^2$. However, in our numerical results as shown in Fig. 3. the central density is observed to increase as v^4 . Hence, it may be that the expansion of Ref. [10] was truncated at a too low order to observe the compression effect described here. The main reason that they could not observe the effect, however, is that the terms involving motion of the central star were discarded. We attribute the compression effect to an enhancement of the self gravity due to the motion of the stars with respect to the corotating frame. Hence, the neglect of terms involving the motion of the central star precludes the possibility of observing the effect.

We believe that the same conclusion is true in the treatments by Refs. [11, 12]. The analysis of Flanagan [11] is based upon the method of matched asymptotic expansion. The metric is approximated

$$g_{\mu\nu} = \eta_{\mu\nu} + h_{\mu\nu}^{NS} + h_{\mu\nu}^B, \quad (39)$$

where the superscript NS refers to the self contribution from one star and B refers to the contribution from a distant companion. The internal gravity of a static neutron star $h_{\mu\nu}^{NS}$ is expanded to all orders. The binary tidal contribution $h_{\mu\nu}^B$ is expanded in powers of the ratio of stellar radius to orbital separation.

First we suggest that such a decomposition may be questionable for a close neutron-star binary. In our metric one can write the metric perturbation as

$$h_{ij} = (\phi^4 - 1) \delta_{ij}. \quad (40)$$

The conformal factor ϕ is a solution to a Poisson equation involving source terms from the two stars. Between the stars, the only source of the fields arises from the $K_{ij}K^{ij}$ terms which are quite small. Hence, neglecting $K_{ij}K^{ij}$ terms, ϕ is additive in the “vacuum” between the stars,

$$\phi = \phi_1 + \phi_2 = 1 + \frac{m_1}{2|r-r_1|} + \frac{m_2}{2|r-r_2|}. \quad (41)$$

Expanding h_{ij} around star 1 in the presence of a distant companion 2 we have

$$\begin{aligned} h_{ij} &= \frac{4}{2} \left(\frac{m_1}{|r-r_1|} + \frac{m_2}{|r-r_2|} \right) + \frac{6}{4} \left(\frac{m_1}{|r-r_1|} + \frac{m_2}{|r-r_2|} \right)^2 + \dots \\ &= h_{\mu\nu}^{NS} + h_{\mu\nu}^B + \text{cross terms}. \end{aligned} \quad (42)$$

However, for the binary systems we have considered, the cross terms are $\sim 15\%$ to 20% of the sum $h_{\mu\nu}^{NS} + h_{\mu\nu}^B$. Hence, they can not be neglected. The errors associated with this decomposition may be part of the reason that the compression effects are not apparent in this work.

A related concern is with the expansion of the stress-energy tensor in [11]. We have noted that most of the compression arises from the net effect of velocity dependent terms in the covariant derivative of the stress-energy tensor. In [11] the stress energy is expanded in powers of the curvature R^{-m} . The author states [11] “We assume initial conditions of vanishing $T_{\mu\nu}^{(2)}$, so that the only source for perturbations is the external tidal field.” An analysis which only considers perturbations from the external tidal field (and not motions of the fluid) will not observe the compression effect. The result of [11] is that the central density is unchanged until tidal forces enter at $O(R^6)$. This is consistent with our results in the limit of only tidal perturbations acting on the stars. It is not clear to us, however, to what degree the velocity dependent terms are included or excluded by this expansion. A more careful recent revision [E. Flanagan, (private communication)] shows an effect coming in a lower order, but not necessarily as strong as we have noted.

In the paper of Thorne [12], a similar tidal expansion is applied. In that work only the stabilizing effect of tidal forces

was considered along with the stabilizing effect of rotation. However, the increased self gravity from velocity-dependent forces was not included. Hence, the conclusions of [12] are consistent with our results based upon tidal forces. So are the Newtonian tidal effects computed in [4].

VI. CONCLUSIONS

The results of this study (cf. Table I) are that we see almost no difference between the central density of an isolated star and a binary star in which rigid corotation has been artificially imposed, or one in which only tidal effects are included. Indeed, in the case of tidal forces alone, the central density in our simulations actually decreases as stars approach, consistent with other works.

An increase in the central density is only apparent in our binary simulations for stars with fluid motion with respect to the corotating frame. (Specifically we considered stars of low intrinsic spin in a binary.) In such cases there is no simple Killing vector which can be imposed to cancel the compression driving forces. We have argued here and in [3] that the main compression effect arises from the net result of velocity-dependent hydrodynamic terms [34]. These terms arise from the affine connection part of the covariant differentiation of the stress-energy tensor.

We show here that the compression effect would not have been observed in a study of tidal forces or any model that artificially imposes rigid corotation of the fluid. A proper treatment must consider all of the force terms apparent in the momentum equation (22) to a sufficient order so that their effects on the fluid self gravity survive. A similar conclusion has been reached in [30] based on test particle dynamics near a Schwarzschild black hole. In that work it is concluded that at least 2.5 post-Newtonian particle dynamics is necessary before a dynamical collapse instability is manifested.

We argue that the results of this study are thus consistent with results in a number of recent papers [4–13] which have analyzed the stability of binary stars in various approximations and limits and see no effect. Since we do not disagree with the lack of a compression effect in the limits that they have imposed, we conclude that the existence or absence of the neutron-star compression effect has not yet been independently tested.

Therefore, if one wishes to explore this effect, it would be best to apply a complete unconstrained strong-field relativistic hydrodynamic treatment employing an EOS which produces realistically compact neutron stars. Another alternative, however, might be to study the quasi-equilibrium structure of nonspinning irrotational binary stars at a sufficiently high order. In this regard a recently proposed formalism [35] to compute quasi-equilibria for nonsynchronous binaries may be of some use. We have begun calculations in this independent formalism. The results will be reported in a forthcoming paper.

Regarding the existence of this low spin state, we find that such a state represents the unconstrained hydrodynamic equilibrium for a close binary. In Newtonian theory, stars are driven to corotation by tidal forces. However in [32] it has been shown that Newtonian tidal forces are insufficient to

produce corotation before the neutron-stars merge unless the viscosity is unrealistically high. Nevertheless, in the absence of strong tidal forces, neutron stars gradually spin down. Therefore, even apart from the hydrodynamic effects described here, stars of low spin are likely to be members of close binaries. The hydrodynamic effects described herein, however, could hasten the spin down as stars approach their final orbits and cause the stars to become more compact.

ACKNOWLEDGMENTS

Work at University of Notre Dame was supported in part by DOE Nuclear Theory grant DE-FG02-95ER40934, NSF grant PHY-97-22086, and by NASA CGRO grant NAG5-3818. Work was performed in part under the auspices of the U. S. Department of Energy by the Lawrence Livermore National Laboratory under contract W-7405-ENG-48 and NSF grant PHY-9401636.

-
- [1] J. R. Wilson and G. J. Mathews, Phys. Rev. Lett. **75**, 4161 (1995).
 - [2] J. R. Wilson, G. J. Mathews, and P. Marronetti, Phys. Rev. D **54**, 1317 (1996).
 - [3] G. J. Mathews and J. R. Wilson, Astrophys. J. **482**, 929 (1997).
 - [4] D. Lai, Phys. Rev. Lett. **76**, 4878 (1996).
 - [5] R. Reith and G. Schäfer (unpublished).
 - [6] A. G. Wiseman, Phys. Rev. Lett. **79**, 1189 (1997).
 - [7] M. Shibata, Prog. Theor. Phys. **96**, 317 (1996); Phys. Rev. D **55**, 6019 (1997); K. Taniguchi and M. Shibata, *ibid.* **56**, 798 (1997); M. Shibata and K. Taniguchi, *ibid.* **56**, 811 (1997); M. Shibata, K. Taniguchi, and T. Nakamura, Prog. Theor. Phys. **128**, 295 (1997).
 - [8] J. C. Lombardi, F. A. Rasio, and S. Shapiro, Phys. Rev. D **56**, 3416 (1997).
 - [9] K. Taniguchi and T. Nakamura, Prog. Theor. Phys. **96**, 693 (1996); D. Lai and A. G. Wiseman, Phys. Rev. D **54**, 3958 (1996); W. Ogawaguchi and Y. Kojima, Prog. Theor. Phys. **96**, 901 (1996).
 - [10] P. Brady and S. Hughes, Phys. Rev. Lett. **79**, 1186 (1997).
 - [11] E. Flanagan, gr-qc/9706045.
 - [12] K. Thorne, Phys. Rev. D (to be published), gr-qc/9706057.
 - [13] T. W. Baumgarte, G. B. Cook, M. A. Scheel, S. L. Shapiro, and S. A. Teukolsky, Phys. Rev. Lett. **79**, 1182 (1997); Phys. Rev. D **57**, 6181 (1998); **57**, 7299 (1998).
 - [14] M. Shibata, T. W. Baumgarte, and S. L. Shapiro, Phys. Rev. D **58**, 023002 (1998).
 - [15] J. R. Wilson, in *Sources of Gravitational Radiation*, edited by L. Smarr (Cambridge University Press, Cambridge, England, 1979), p. 423.
 - [16] R. Arnowitt, S. Deser, and C. W. Misner, in *Gravitation*, edited by L. Witten (Wiley, New York, 1962), p. 227.
 - [17] J. W. York, Jr., in *Sources of Gravitational Radiation*, edited by L. Smarr (Cambridge University Press, Cambridge, England, 1979), p. 83.
 - [18] C. R. Evans, Ph.D. thesis, University of Texas, 1985.
 - [19] G. B. Cook, M. W. Choptuik, M. R. Dubal, S. Klasky, R. A. Matzner, and S. R. Oliveira, Phys. Rev. D **47**, 1471 (1993).
 - [20] B. Brüggmann, Phys. Rev. Lett. **78**, 3606 (1997).
 - [21] P. Anninos, D. Hobill, E. Seidel, and L. Smarr, Phys. Rev. Lett. **71**, 2851 (1993).
 - [22] A. M. Abrahams, in *Sixth Marcel Grossmann Meeting, Kyoto 1991*, edited by H. Sato, and T. Nakamura (World Scientific, Singapore, 1992), p. 345.
 - [23] C. W. Misner, K. S. Thorne, and J. A. Wheeler, *Gravitation* (Freeman, San Francisco, 1973).
 - [24] K. S. Thorne, Rev. Mod. Phys. **52**, 299 (1980).
 - [25] D. Kramer, H. Stephani, E. Herlt, and M. MacCallum, in *Exact Solutions of Einstein's Field Equations*, edited by E. Schmutzer (Cambridge University Press, Cambridge, England, 1980).
 - [26] L. P. Eisenhart, *Riemannian Geometry* (Princeton University Press, Princeton, New Jersey, 1996).
 - [27] G. B. Cook, S. L. Shapiro, and S. A. Teukolsky, Phys. Rev. D **53**, 5533 (1996).
 - [28] J. W. York, Jr., J. Math. Phys. **14**, 456 (1973).
 - [29] T. Nakamura (private communication).
 - [30] S. L. Shapiro, Phys. Rev. D **57**, 1084 (1998).
 - [31] P. Marronetti, G. J. Mathews, and J. R. Wilson, gr-qc/9803093.
 - [32] L. Bildsten and C. Cutler, Astrophys. J. **400**, 175 (1992).
 - [33] J. R. Wilson and G. J. Mathews (unpublished).
 - [34] Although in [3] we pointed out that velocity dependent corrections enter into the source for the post-Newtonian potential this was for illustration and not identification of the main effect.
 - [35] S. Bonazzola, E. Gourgoulhon, and J.-A. Marck, Phys. Rev. D **56**, 7740 (1997); S. A. Teukolsky, gr-qc/9803082 (1998); M. Shibata, Phys. Rev. D **58**, 024012 (1998); E. Gourgoulhon, Phys. Rev. D (to be published), gr-qc/9804054, 1998.